# Quantitative Scanning Electron Microscopy

D. B. HOLT, M. D. MUIR,

P. R. GRANT and I. M. BOSWARVA

# Quantitative Scanning Electron Microscopy

*Edited by*

**D. B. HOLT, M. D. MUIR,**

**P. R. GRANT and I. M. BOSWARVA**

*Imperial College of Science and Technology,*
*London, England*

1974

ACADEMIC PRESS

London New York San Francisco

*A Subsidiary of Harcourt Brace Jovanovich, Publishers*

ACADEMIC PRESS INC. (LONDON) LTD.
24/28 Oval Road,
London NW1

*United States Edition published by*
ACADEMIC PRESS INC.
111 Fifth Avenue
New York, New York 10003



Library of Congress Catalog Card Number: 745645
ISBN: 0-12-353850-5

PRINTED IN GREAT BRITAIN AT
THE UNIVERSITY PRESS, ABERDEEN

# Preface

In the decade since commercial scanning electron microscopes first became available, the modes of operation and the applications have expanded rapidly. Initially, attention was confined almost exclusively to the exploitation of the special features of secondary emission. Micrographs of such emission compare with those obtained by reflected light microscopy, but have inherently a much greater depth of focus and even in the earliest instruments, a point to point resolution better than the best optical microscope. Among the earlier accessories were specimen current amplifiers and picture manipulating modules. Very rapidly, modes of operation such as selected area diffraction, cathodoluminescence, scanning transmission, voltage contrast and X-ray analysis became commonly ancillary, if not, in some cases, dominant.

These innovations were realized quite early in the history of the commercial scanning electron microscopes. Thus with the basic hardware available latterly, there has been a marked trend toward the development of empirical and theoretical methods for the quantitative interpretation of the wide range and vast amount of information available from multi-mode scanning electron microscopes.

This book collates accounts of the current state of development of quantitative scanning electron microscopy. Many leading authorities in this field have contributed not only statements of the present level of development but also their views on the directions and form of future advances.

A number of chapters arose from lectures given at an Advanced Summer School on Scanning Electron Microscopy held at Imperial College. Others were specifically requested contributions which we found necessary to round out certain aspects or to act as links between sections.

Although we have aimed at the adoption of an acceptable set of common symbols throughout, this has not been wholly achieved. However, lists of symbols and, for easy reference, of contents precede each chapter, and relevant references are listed at the end of each chapter.

In an attempt to ensure that this book will be useful for teaching and for study, though an acquaintance with the basic features of the scanning electron microscope is assumed, the treatment herein is relatively complete, consecutive and, we hope, comprehensible.

Special emphasis has been given to new developments and new instruments. Because of their recent development and potential, three chapters have been devoted to electron channelling and Kossel patterns. In contrast, electron probe analysis using crystal spectrometers has long been at a high level of development and has therefore only been summarized in a single chapter. However, references to the standard literature make this latter chapter complete.

We believe that future developments will increasingly be concerned with electronic signal processing and computer analysis of SEM data. Therefore, we have included chapters on image analysis by computer, on energy dispersive X-ray spectrometers and the employment of multichannel analysis in such instruments, and on automatic computer controlled point analysis, and stereological analysis in the X-ray mode. We hope that this book will be found valuable by expert and novice scanning electron microscopists alike.

Much thought and effort has been given to the preparation of this volume by the individual authors, whom we would like to thank for their prompt and conscientious work.

We would like to thank Professor J. G. Ball for his interest in this project in particular and together with Professor J. Sutton for support and encouragement for scanning electron microscopy at Imperial College.

*June*, 1974

D. B. Holt
M. D. Muir
P. R. Grant
I. M. Boswarva

# Contents

## Contributors

J. A. BELK *Metallurgy Branch, The Royal Military College of Science, Shrivenham, Swindon, Wiltshire, England.* (p. 389)

H. E. BISHOP *Materials Development Division, Atomic Energy Research Establishment, Harwell, England.* (p. 41)

A. V. CREWE *The University of Chicago, Chicago, Illinois, U.S.A.* (p. 65)

D. J. DINGLEY, *H. H. Wills Physics Laboratory, University of Bristol, England.* (p. 487)

D. A. GEDCKE *ORTEC Inc., Oak Ridge, Tennessee, U.S.A.* (p. 403)

D. W. GIBBARD *Image Analysing Computers Ltd., Melbourn, Royston, Hertfordshire, England.* (p. 75)

A. GOPINATH *School of Electronic Engineering Science, University College of North Wales, Bangor, Caernarvonshire, North Wales.* (p. 95)

P. R. GRANT *Department of Geology, Imperial College of Science and Technology, Prince Consort Road, London S.W.7, England.* (p. 287)

D. B. HOLT *Department of Metallurgy, Imperial College of Science and Technology, Prince Consort Road, London S.W.7, England.* (pp. 213, 335)

A. HOWIE *Cavendish Laboratory, University of Cambridge, England.* (p. 183)

*B. JEFFERIES *Department of Mineralogy and Petrology, University of Cambridge, England.* (p. 517)

M. P. JONES *Department of Mineral Technology, Imperial College of Science and Technology, Prince Consort Road, London S.W.7, England.* (p. 531)

D. C. JOY *Department of Metallurgy, University of Oxford, England.* (p. 131)

J. V. P. LONG *Department of Mineralogy and Petrology, University of Cambridge, England.* (p. 517)

M. D. MUIR *Department of Geology, Imperial College of Science and Technology, Prince Consort Road, London S.W.7, England.* (pp. 3, 287)

J. W. STEEDS *H. H. Wills Physics Laboratory, University of Bristol, England.* (p. 487)

H. YAKOWITZ *Metallurgy Division, Institute for Materials Research, National Bureau of Standards, Washington, D.C., U.S.A.* (p. 451)

* Present address: *Department of Geology, University of Edinburgh, Scotland.*

PART I

# Instrumental

*Chapter 1*

# Recent Instrumental Developments

M. D. MUIR

*Geology Department, Royal School of Mines, London, England*



## Symbols

$J$ = the current density in the image
$J_0$ = the current density at the cathode surface
$e$ = the electronic charge
$V$ = potential difference between the cathode and the point where the image is formed
$k$ = Boltzmann's constant
$T$ = absolute temperature in the cathode
$\alpha$ = the semi-angle of the cone of rays which converge to form a point on the image
$\beta$ = the useful current density in the crossover—the brightness of the source
$V_p$ = the voltage at the crossover
$d_0$ = the Gaussian probe size, i.e. the total demagnification of the beam's first crossover
$C_s$ = the spherical aberration coefficient of the final lens
$\alpha_1$ = the beam semiangle of convergence at the first crossover
$C_c$ = the chromatic aberration coefficient of the final lens
$E_0$ = the mean energy of the beam
$\delta E_0$ = the energy spread of the beam passing through the lens
$\delta z$ = the spacing of the two stigmatic foci
$\lambda$ = the de Broglie wavelength of the electrons
$\alpha_i$ = the half angle of convergence of the beam at the specimen
$C_s\alpha_1^3$ = the diameter of the disc of least confusion due to the use of lenses with finite numerical apertures
$I_b$ = the incident probe current
$d_{\min}$ = the minimum probe diameter
$A$ = a constant approximately equal to one
$T_s$ = picture exposure time

$N$ = number of lines in square picture (field of view)
$c$ = fractional threshold contrast
$R_V$ = radius of the virtual cathode source
$R$ = actual radius of the tip
$E_t$ = average transverse energy of electrons leaving the tip
$V_1$ = voltage between the tip and first anode
$V_0$ = the desired potential of the gun
$E_s$ = field enhancement factor due to the effective lowering of the potential barrier—the Schottky effect
$\phi$ = the work function
$F$ = electric field magnitude (V cm$^{-1}$)
$J_F$ = cathode current density for field emission
$J(T)$ = cathode current density at temperature $T$
$\Delta E_{tot}$ = total energy distribution in the final beam
$\Delta E_{th}$ = thermal energy spread
$\Delta E_{interact}$ = Boersch effect
subscript $d$ = diffraction disc
subscript $c$ = chromatic aberration
$E$ = total energy
$d_{CT}$ = limit of CTEM resolution
$\bar{d}(t)$ = limit of resolution in a specimen of thickness $t_0$
$d_{eff}$ = effective beam diameter
$d_s$ = multiple scattering
$d_f$ = depth of focus
$d_c$ = chromatic scatter
$t$ = depth of structure of interest in specimen
$M$ = mass of coating material of density $\rho$
$T_f$ = film thickness in nm
$R$ = distance in cm from evaporation source to sample
$\upsilon$ = angular deviation from the normal of the source to specimen surface
$\sigma(t)$ = surface charge density at time $t$
$\sigma(0)$ = surface charge density at time zero assumed = zero
$\sigma_m$ = maximum surface charge density
$\eta_r$ = specimen resistivity
$\varepsilon$ = specimen permittivity
$M_g$ = magnification
$\beta_{SE}$ = secondary emission coefficient
$A_v$ = area of visual display
$\eta$ = backscattering coefficient
$\mathscr{V}$ = a hole created by electron impact
$X$ = a higher level
$Y$ = a lower energy
$E_\mathscr{V}$ = the energy level of the initial hole
$E_\mathscr{X}$ = the binding energy at level $X$
$E_\mathscr{Y}$ = the binding energy at level $Y$
$\bar{a}_\mathscr{V}$ = the mean Auger yield
$\bar{\omega}_\mathscr{V}$ = the X-ray fluorescence yield

## I. Introduction

This book is intended as a summary of present understanding of quantitative scanning electron microscopy; for introductory accounts of scanning microscopes, their operation, and reviews of their applications in particular fields, reference must be made elsewhere.

An introductory account of the field is given by Thornton (1968), and Oatley (1972) describes the instrument, its design and the factors limiting its performance. The proceedings of the annual SEM Symposia held at the Illinois Institute of Technology (SEM 1968 through SEM 1974) provide a useful starting point for entry into the detailed SEM literature and the volumes contain bibliographies of the whole field of SEM investigations.

Here I have tried to summarize the rapid evolution of the instrument in recent years and to introduce the considerations involved in intercomparing the related techniques of scanning transmission electron microscopy (STEM) and conventional transmission electron microscopy (CTEM). These topics are further dealt with in Chapters 3 and 7 below.

## II. The Scanning Electron Microscope

Although the scanning electron microscope (SEM) has as long a history as the transmission electron microscope (CTEM) both instruments being derived from the laboratories of Knolle and Ruske (Zworykin, Hillier and Snyder, 1942), its real development and exploitation began after the development of the electron probe family of instruments (Castaing, 1951). These are basically bipartite instruments: they comprise two systems with the specimen at the interface. The electron optical column provides the scanned electron beam "illumination" of the specimen. The second section of the SEM comprises at minimum a signal collection and display system. This section may be expanded for quantitative work into a signal detection, amplification, data processing and read-out system. Recent developments in instrumentation for the first section of the microscope are discussed in this chapter. The remainder of the book is devoted to the various quantitative aspects of the second section of the SEM.

In the earliest electron probe instruments, the electron beam did not scan. This was because the prime function of these instruments was the generation of X-rays for elemental analysis in metallurgical and mineralogical specimens. The X-rays were emitted from a volume near the specimen surface and could be diffracted by a crystal spectrometer on the Rowland Circle. Knowledge of the conditions limiting Bragg reflections of the X-rays from the diffracting crystal enables a quantitative determination to be made of the element present in the excited volume of the specimen. Moving the crystal round the Rowland circle enables X-rays of different wavelengths and hence different elements to be identified. The geometry of the take-off angle of the X-rays is critical and for quantitative electron probe microanalysis depends upon having the angle of incidence of the electron beam precisely normal to the specimen surface. Because of these geometric limitations, it was advantageous for Castaing (1951; also Castaing and Guinier 1949) to use a static electron beam in his electron probe.

However useful point analyses may be, it is obviously faster to be able to look at relatively large areas of the specimen surface, and electron probes designed after 1959 (Cosslett and Duncumb, 1956; Duncumb

and Melford, 1959) all possess scanning coils in the electron optical system. The beam scans in a raster or square, and by scanning a larger or smaller area, the ultimate signal from the specimen gives a lower or higher magnification when enlarged to a constant size in the display system. The later electron probes could also use the single element X-ray output to generate the display signal, thus enabling distribution maps of single elements to be produced.

The other elements of the electron optical column of the SEM are to be found in the CTEM as well as the electron probe. The electron source is still commonly a thermionic tungsten filament in an electron gun. In such a gun, the electrons are emitted from a cathode, and accelerated by a field produced by the anode, usually at a positive potential in the order of 1 kV with respect to the cathode. A third electrode lies between the anode and the cathode and is negative in potential with respect to the cathode (Fig. 1). This last electrode is generally described as the Wehnelt electrode (or grid, or modulator).

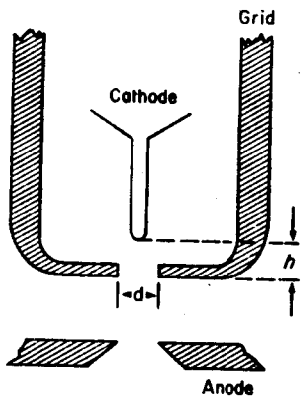


FIG. 1. Diagram of a triode gun with a tungsten hairpin filament. $d$ = the aperture in the Wehnelt electrode (called the Grid in the diagram); $h$ = filament height from the Wehnelt. (After Haine and Einstein, 1952.)

This gun, the triode gun, is assumed to have a planar filament, and electrons leaving different point sources along the filament have a Maxwellian distribution of initial velocities which causes them to crossover at a point beyond the anode. This crossover can be regarded as a small electron source, and the demagnified image of this crossover forms the electron probe impinging on the specimen. The useful current density in the crossover is given by $\beta$—the maximum permitted brightness

according to Langmuir's Law (1937) which gives for the upper limit of the current density in the image:

$$J = J_0[(eV/kT)+1] \sin^2\alpha \tag{1}$$

where

$J$ = the current density in the image
$J_0$ = the current density at the cathode surface
$e$ = electronic charge
$V$ = potential difference between the cathode and the point where the image is formed
$k$ = Boltzmann's constant
$T$ = absolute temperature of the cathode
$\alpha$ = the semi-angle of the cone of rays which converge to form a point on the image.

$\beta$ is expressed in units of amps per square metre per steradian and can be calculated from the following equation (Oatley, 1972):

$$\beta = J_0 eV_p/\pi kT \tag{2}$$

where $V_p$ is the voltage at the crossover.

The image of the crossover region is demagnified through (usually) three magnetic lenses, although electron probes and some commercial SEMs use two. As with any type of magnetic lens, those in the SEM are subject to spherical and chromatic aberrations and astigmatism. However, since all the lenses are demagnifying, only the aberrations of the final lens need be taken into account (Joy, 1973) and the probe size actually obtained, $d$, may be written as:

$$d^2 = d_0^2+(\tfrac{1}{2}C_s\alpha_1^3)^2+\left(C_c\alpha_1\frac{\delta E_0}{E_0}\right)^2+(\alpha_1\delta z)^2+\left(\frac{1{\cdot}22\lambda}{\alpha_i}\right)^2 \tag{3}$$

where

$d_0$ = the Gaussian probe size, i.e. the total demagnification of the beam's first crossover;
$C_s$ = the spherical aberration coefficient of the final lens;
$\alpha_1$ = the semiangle of convergence of the beam on the first crossover;
$C_c$ = the chromatic aberration coefficient of the final lens;
$E_0$ = the mean energy of the beam;
$\delta E_0$ = the energy spread of the beam passing through the lens;
$\delta z$ = the spacing of the two stigmatic foci;

$\lambda$ = the de Broglie wavelength of the electrons which is inversely proportional to the square root of the energy of the beam;

$\alpha_i$ = the half angle of convergence of the beam at the specimen;

and

$C_s\alpha_1^3$ = the diameter of the disc of least confusion due to the use of lenses with finite numerical apertures;

$\frac{1{\cdot}22\lambda}{\alpha_i}$ = the diameter of the disc of least confusion as limited by diffraction considerations;

$\delta z\alpha_i$ = the diameter of the disc of least confusion when astigmatic factors are minimized.

$\frac{C_c\delta E_0\alpha}{E_0}$ = the diameter of the disc of least confusion when the high voltage supplies are not perfectly stable and lenses are not perfect thus causing a spread of energies of the beam about a mean value.

In a well set up microscope, the chromatic and astigmatic contributions are negligible compared with the other factors, and the equation can be simplified to:

$$d^2 = d_0^2+(\tfrac{1}{2}C_s\alpha_1^3)^2+\left(\frac{1{\cdot}22\lambda}{\alpha_i}\right)^2 \tag{4}$$

The incident probe current is given by:

$$I_b = 2{\cdot}5\beta\alpha_1^2d^2-(\tfrac{1}{2}C_s\alpha_1^3)^2-\left(\frac{1{\cdot}22\lambda}{\alpha_i}\right)^2 \tag{5}$$

and thus it is clear that use of too small a probe size may give a probe current insufficient for the purpose for which the SEM is to be used.

## III. Electron Sources

At the time of writing, there are two basically different types of electron source. The first of these is the thermionic emitter, and the most commonly used version of thermionic cathode is the tungsten hairpin. This is operated by heating the filament directly by passing a current through it. This activates a few of the electrons near the Fermi surface to a sufficiently high energy to enable them to escape over the surface potential barrier. The thermionic gun is usually of a triode design as described above. However, in recent years, pointed filaments,

i.e. solid rods of a suitable material, fabricated to a fine point have been used, with some advantages becoming apparent. Tungsten pointed filaments are available, but offer no very great advantage over the hairpin type of filament because of their high work function. Plomp (1972) gives a table which shows the work function for various potential cathode materials (Table I) and it is clear that tungsten is very considerably worse then the other materials considered.

TABLE I.

| Compound | Melting point (°C) | Work function (V) |
|---|---|---|
| $YB_6$ | 2300 | 2·2 |
| $LaB_6$ | 2200 | 2·7 |
| ZrC | 3530 | 3·2 |
| TaC | 3800 | 3·2 |
| W | 3370 | 4·5 |

(After Plomp, 1972.)

This factor led several workers to consider some of these other emitters as possible cathodes, and Broers (1969) described the experimental and estimated characteristics of a lanthanum hexaboride rod type of electron gun. This gun gave an appreciable gain in brightness, and because it, therefore, gave a larger number of electrons in a small spot size, better resolving power became possible because of the improved signal to noise ratio.

Further developments of this type of gun have been reported by Ahmed (1972) who shows how not only gun brightness but rod lifetime have been greatly improved (Fig. 2). Ahmed and Nixon (1973) describe how different boride guns give better performances compared with the conventional tungsten hairpin gun.

An unusual development of the heated cathode is the indirectly heated cathode of le Poole *et al.* (1972). Their cathode is a thin, straight tungsten wire a small fraction of which is indirectly heated by an electron beam to a temperature just below the melting point. At this much higher temperature, 3500°K compared with the normal emission temperature of 2800°K, much more efficient emission can take place. They have contrived an ingenious mechanical device for moving the filament away from the heating electron beam after it has reached a critical thickness, and it is possible that this type of gun, which requires only

normal vacuum and operating conditions may be used in the SEM of the future.

Thermionic cathodes can be operated in a vacuum of about $10^{-5}$ Torr, for the tungsten hairpin type, and a vacuum of $10^{-6}$–$10^{-7}$ Torr for the pointed rod $LaB_6$ type cathodes. The second important type of electron source, the field emission source, suffers from the disadvantage that it will only operate under ultra-high vacuum conditions, typically $5 \times 10^{-10}$ Torr or better, and this leads inevitably to difficulties in microscope design and operation. However, this type of source has many advantages when compared with the thermionic cathode, and most manufacturers are pressing on with development of field emission guns for commercial SEMs.

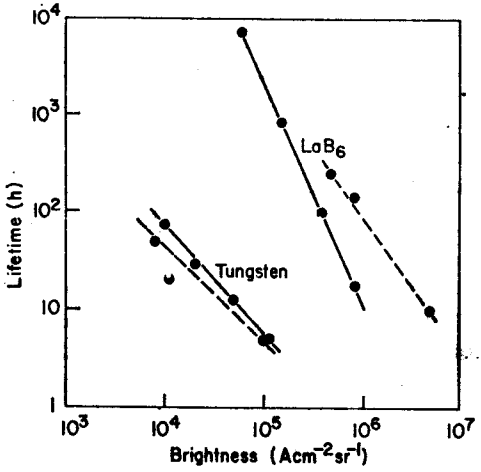


FIG. 2. Comparison of a tungsten hairpin filament with a $LaB_6$ rod cathode. Brightness is plotted against lifetime, and in the case of the $LaB_6$ cathode, the experimental results are better than those calculated theoretically. (After Ahmed, 1972.)

In its simplest form, the field emission gun is a two electrode or diode gun. Figure 3 (Smith, 1972) is a schematic diagram of such a gun. If a voltage of 1–3 kV is applied between the surface of the emitter, usually a crystallographically oriented tungsten rod with a tip radius about 200 Å, and the anode, a field is produced at the emitter surface which gives rise to emission by tunnelling through the potential barrier. The emission current density produced in this way is extremely high compared with that produced by thermionic emission. It is also non-uniform, being strongly influenced by the crystallographic orientation of the emitter at the point of emission, and certain orientations, e.g.